Anharmonic Oscillator. II. A Study of Perturbation Theory in Large Order

Carl M. Bender*
Department of Mathematics, Massachusetts Institute of Technology, Cambridge, Massachusetts 02139

and

Tai Tsun Wu†
Gordon McKay Laboratory, Harvard University, Cambridge, Massachusetts 02138
(Received 21 August 1972)

This paper is concerned with the nature of perturbation theory in very high order. Specifically, we study the Rayleigh-Schrödinger expansion of the energy eigenvalues of the anharmonic oscillator. We have developed two independent mathematical techniques (WKB analysis and difference-equation methods) for determining the large-n behavior of A_n^K, the nth Rayleigh-Schrödinger coefficient for the Kth energy level. We are not concerned here with placing bounds on the growth of A_n^K as n, the order of perturbation theory, gets large. Rather, we consider the more delicate problem of determining the precise asymptotic behavior of A_n^K as $n \to \infty$ for both the Wick-ordered and non-Wick-ordered oscillators. Our results are in exact agreement with numerical fits obtained from computer studies of the anharmonic oscillator to order 150 in perturbation theory.

I. INTRODUCTION

This paper reports an intensive study of the behavior of perturbation theory in very high order for the anharmonic oscillator.[1] We give a detailed treatment of the new mathematical techniques we have developed to obtain this behavior and we discuss the related physical ideas.

The quantum anharmonic oscillator is described by the time-independent Schrödinger equation

$$\left[\frac{d^2}{dx^2} + \frac{x^2}{4} + \frac{\lambda x^4}{4} - E(\lambda)\right]\psi(x) = 0 \tag{1.1}$$

with the associated boundary condition

$$\lim_{|x| \to \infty} \psi(x) = 0 . \tag{1.2}$$

The boundary condition selects out a discrete set of energy eigenvalues $E^K(\lambda)$, $K = 0, 1, 2, \ldots$, whose perturbation expansions take the form

$$E^K(\lambda) \sim K + \tfrac{1}{2} + \sum_{n=1}^{\infty} A_n^K \lambda^n . \tag{1.3}$$

We refer to Eq. (1.3) as the Rayleigh-Schrödinger series and A_n^K as a Rayleigh-Schrödinger coefficient. We investigate the behavior of A_n^K as n, the order of perturbation theory, becomes large.

The anharmonic oscillator is also expressible as a $(\lambda\phi^4)_1$ quantum field theory.[2] The Hamiltonian for the theory may be written as

$$H = \tfrac{1}{2}\dot{\phi}^2 + \tfrac{1}{2}m^2\phi^2 + \lambda\phi^4 , \tag{1.4}$$

where

$$[\phi, \dot{\phi}] = i . \tag{1.5}$$

The energy levels $E^K(\lambda)$ are the eigenvalues of H:

$$H|K\rangle = E^K(\lambda)|K\rangle . \tag{1.6}$$

For all m, the field-theoretic perturbation series takes the form

$$E^K(\lambda) \sim m\left(K + \tfrac{1}{2} + \sum_{n=1}^{\infty} A_n^K (\lambda m^{-3})^n\right). \tag{1.7}$$

One can recover Eq. (1.3) by setting $m = 1$ in Eq. (1.7).

Viewing the anharmonic oscillator as a quantum field theory, we can express A_n^K in terms of Feynman diagrams.[3] A_n^0 is the sum of all connected diagrams having n vertices and no external legs. A_n^K is the K-particle pole of the $2K$-point Green's function. Thus, the problem of determining the large-n behavior of A_n^K corresponds to studying diagrams with many vertices. There has already been an intensive study of the properties of many-vertex diagrams in higher-dimensional quantum field theory[4] as well as in the anharmonic oscillator.[5] However, these studies give only bounds on the growth of the Rayleigh-Schrödinger coefficients and do not reveal much about the mathematical and physical nature of these theories. In this paper we completely by-pass the problem of obtaining bounds. Instead, we solve here the much more formidable problem of determining the precise asymptotic behavior of A_n^K for large n.

This paper will conform to the following outline: In Sec. II we use dispersion techniques to derive an exact relation between the nth Rayleigh-Schrödinger coefficient and the lifetimes of the unstable states of a negatively coupled anharmonic oscillator ($\lambda = -\epsilon$, $\epsilon > 0$). Section III contains a WKB derivation of approximate lifetimes for small ϵ. In Sec. IV we combine the results of Secs. II and III to find the leading behavior of A_n^K for large n. In Sec. V we discuss the relation between the WKB analysis of Sec. III and other WKB results we obtained in a previous paper. Then we compute the corrections (of order n^{-1}) to the leading behavior of A_n^K given in Sec. IV. A completely independent derivation of the results of Sec. IV for the two lowest energy levels is given in Sec. VI. This derivation uses difference-equation and generating-function methods. Finally, in Sec. VII we define and discuss the large-order perturbation behavior of the Wick-ordered version of the Hamiltonian in Eq. (1.4). The Appendix gives a short and physically intuitive derivation of the material in Sec. III.

The results of this paper may be summarized in two equations. For large n,

$$A_n^K = \frac{(-1)^{n+1}12^K\sqrt{6}}{K!\,\pi^{3/2}}\, 3^n\Gamma(n+K+\tfrac{1}{2}) \times\left[1 - \frac{1}{n}\left(\frac{95}{72}+\frac{29K}{12}+\frac{17K^2}{12}\right)+O(n^{-2})\right] \tag{1.8}$$

and

$$\frac{A_n^K}{B_n^K} = e^{-3}\left(1 + \frac{1+3K}{n} + \frac{\frac{71}{6}+31K+23K^2}{4n^2} + O(1/n^3)\right), \tag{1.9}$$

where B_n^K is a Rayleigh-Schrödinger coefficient for the Wick-ordered perturbation series. These results have been verified: On a computer we have carried out perturbation theory to order $n = 150$ (the limiting factor is the amount of available core memory), performed numerical fits,[6] and obtained spectacular agreement.

In this paper we have established an easily generalized mathematical framework for determining the large-order behavior of perturbation theory for more complicated models. Three such models have already been successfully investigated: The anharmonic oscillator with a λx^{2N} perturbation,[7] the anharmonic oscillator with an arbitrary polynomial interaction of the form[8]

$$\lambda(x^{2n} + ax^{2N-2} + bx^{2N-4} + cx^{2N-6} + \cdots),$$

and the N-mode problem (N-coupled anharmonic oscillators).[9] This last problem involves applying WKB methods to partial differential equations and is thus far more difficult and profound than the problem considered here. We hope to extend these methods to infinite-mode problems and thereby obtain results for higher-dimensional quantum field theories.

II. DISPERSION RELATION FOR $E^K(\lambda)$

In this section we use a once-subtracted dispersion integral to establish an exact relation between A_n^K, the nth Rayleigh-Schrödinger coefficient for the Kth energy level, and the lifetime of the Kth (unstable) state of a negatively-coupled anharmonic oscillator. This relation follows from three rigorous properties of $E^K(\lambda)$ in the cut λ plane (cut along the real λ axis from $-\infty$ to 0): (a) $|E(\lambda)| \sim |\lambda|^{1/3}$ as $|\lambda| \to \infty$; (b) $E(\lambda)$ is analytic; and (c) the series in Eq. (1.3) is asymptotic. Property (a) is a consequence of a simple scaling argument known as the Symanzik transformation applied to Eq. (1.1).[10] Property (b) is a profound result obtained by Loeffel and Martin.[11] Property (c) was established by Loeffel, Martin, Simon, and Wightman.[12]

Properties (b) and (c) were originally established heuristically by us.[13] They follow directly from a study of Eqs. (1.1) and (1.2) in the complex x plane. The boundary condition Eq. (1.2) holds in a pair of sectors of angular opening $\frac{1}{3}\pi$ centered about the real x axis. As λ rotates into the complex λ plane ($\arg\lambda$ increases from 0), the sectors rotate clockwise. (A full description of the rotating sectors is given in BW.) The distant turning points[2] at $x_1 \sim \pm i\lambda^{-1/2}$ rotate clockwise and faster than the sectors rotate. The turning points enter the sector when $\arg\lambda = \pi$ (λ is negative). When $\arg\lambda < \pi$ WKB methods[2] give the asymptotic series in Eq. (1.3). When $\arg\lambda > \pi$ the WKB results are completely different[2] and predict nonanalyticity (branch points at which level crossing occurs) of $E^K(\lambda)$ in the λ plane. Thus, at $\arg\lambda = \pi$ (and $-\pi$), the distant turning point which enters the sector marks the edge of the region in the λ plane where the series in Eq. (1.3) is asymptotic and where the nonanalyticity of $E(\lambda)$ appears. While not rigorous, these are strong arguments for the truth of properties (b) and (c).

We proceed to derive the dispersion relation. Properties (a), (b), and (c) motivate the definition

$$F^K(\lambda) \equiv [E^K(\lambda) - K - \tfrac{1}{2}]\lambda^{-1}. \tag{2.1}$$

In the cut λ plane, $F^K(\lambda)$ is analytic and

$$\lim_{|\lambda|\to 0} \lambda F(\lambda) = 0, \tag{2.2}$$

$$|F^K(\lambda)| \sim |\lambda|^{-2/3} \quad \text{as} \quad |\lambda| \to \infty. \tag{2.3}$$

Equation (2.2) is a consequence of property (c).

Since $F^K(\lambda)$ is analytic in the cut λ plane, we use the Cauchy theorem to write

$$F^K(\lambda) = \frac{1}{2\pi i}\oint_C \frac{F^K(x)}{x-\lambda}\,dx. \tag{2.4}$$

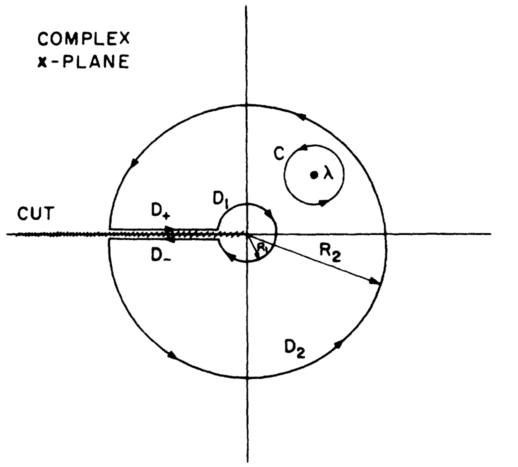

FIG. 1. Change of contour in the x plane used to derive the dispersion relation in Eq. (2.5).

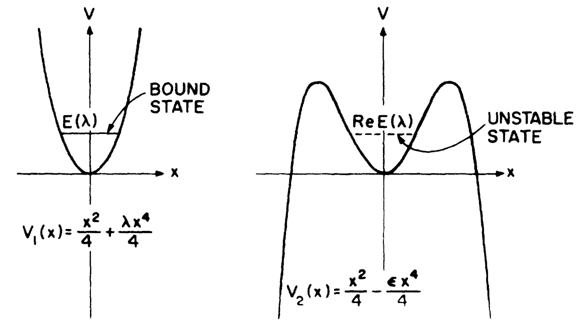

FIG. 2. Comparison of potentials having positive and negative anharmonic terms.

The contour C may be shifted to the contour $D=D_+ + D_- + D_1 + D_2$ (see Fig. 1). Letting $R_1 \to 0$ and $R_2 \to \infty$, the contributions from the curves D_1 and D_2 vanish as a consequence of Eq. (2.2) and (2.3). Thus,

$$F^K(\lambda)=\frac{1}{2\pi i}\int_{-\infty}^{0}\frac{D^K(x)}{x-\lambda}dx\,, \tag{2.5}$$

where

$$D^K(x)\equiv\lim_{\epsilon\to 0}\left[F^K(x+i\epsilon)-F^K(x-i\epsilon)\right]. \tag{2.6}$$

Equation (2.5) is the once-subtracted dispersion relation we have sought.

Finally, we insert the identity

$$\frac{1}{x-\lambda}=\sum_{n=0}^{\infty}\frac{\lambda^n}{x^{n+1}}$$

into Eq. (2.5), compare the resulting series in powers of λ with that in Eq. (1.3), and obtain

$$A_n^K=\frac{1}{2\pi i}\int_{-\infty}^{0}D^K(x)x^{-n}\,dx\,. \tag{2.7}$$

Equation (2.7) is an exact and rigorous result.[14]

Physically, the relation in Eq. (2.7) may be understood by comparing two potentials with positive and negative anharmonic terms:

$$V_1(x)=\frac{x^2}{4}+\frac{\lambda x^4}{4},\quad \lambda>0$$

$$V_2(x)=\frac{x^2}{4}-\frac{\epsilon x^4}{4},\quad \epsilon>0\,.$$

These potentials are shown on Fig. 2. The first potential has bound states. The second potential has only unstable states (having complex energy). If ϵ is very small, the real part of the energy of an unstable state of V_2 is approximately equal to the energy of the corresponding bound state of V_1. $\mathrm{Im}E(\epsilon)$ is very small and is related to the lifetime of the state which is very long. Equation (2.7) relates the Rayleigh-Schrödinger coefficients of the perturbation expansion of $E(\lambda)$ to the inverse moments of $\mathrm{Im}E(\epsilon)$.

Equation (2.7) is the basis for most of the approximations used in this paper. When n is very large, the contribution to the integral in Eq. (2.7) comes entirely from the region near $x=0$. Thus, it is necessary to compute approximately $\mathrm{Im}E(\epsilon)$ for small ϵ. This will be done in the next section using WKB techniques.

III. WKB ZEROTH ORDER AT $\arg\lambda=\pi$

In the previous section it was shown that the large-order behavior of the perturbation series for $E^K(\lambda)$ depends on the imaginary part of the energy for negative coupling constant. In this section we use WKB techniques to calculate $\mathrm{Im}E^K(\epsilon)$ to lowest order in powers of ϵ, where

$$\epsilon=-\lambda>0\,. \tag{3.1}$$

Until now, WKB approximations to $E(\lambda)$ have been given for every value of $\arg\lambda$ except for $\arg\lambda=\pi$.[2] Well-known technical problems, such as the phenomenon of subdominance, associated with transmission through a potential barrier,[15] make this calculation an order of magnitude more difficult than all previous ones. However, we will show how, with extreme care, one may avoid the ambiguities of this transmission problem.

$E^K(\epsilon)$ is defined by the differential equation

$$\left[-\frac{d^2}{dx^2}+\frac{x^2}{4}-\epsilon\,\frac{x^4}{4}-E^K(\epsilon)\right]\Phi(x)=0\,. \tag{3.2}$$

Equation (3.2) describes a particle in a potential well in a slightly unstable state (very long half-life). As ϵ becomes smaller, the lifetime of the state increases because the particle must pass through a higher potential barrier to escape. Thus, $\mathrm{Im}E^K(\epsilon)$, which goes as the reciprocal of the lifetime, is extremely small.

The wave function $\Phi(x)$ satisfies two boundary conditions. At the origin,

$$\Phi(0)=0 \text{ for odd-parity states}, \tag{3.3a}$$

$$\Phi'(0)=0 \text{ for even-parity states}. \tag{3.3b}$$

At $x=+\infty$, the boundary conditions are somewhat complicated because at first glance they seem to be undefined. It would appear that any linear combination of outgoing waves and incoming waves, $\exp(\pm i\epsilon^{1/2}x^3/6)$, would suffice. However, we recall that the analytic continuation of the energy levels into the complex λ plane is accomplished by simultaneously rotating x into the complex x plane.[2] When $\arg\lambda=\pi$, the sector in which the boundary condition, $\lim_{|x|\to\infty}\psi(x)=0$, applies is given by $-\frac{1}{3}\pi<\arg(\pm x)<0$. Thus it is necessary to pick that asymptotic behavior which vanishes exponentially if the argument of x lies between $0°$ and $-60°$. Hence, $\Phi(x)$ must obey the boundary condition

$$\Phi(x)\sim\left(\frac{\text{const}}{x}\right)e^{-i\epsilon^{1/2}x^3/6} \text{ as } x\to+\infty. \tag{3.4}$$

For small ϵ the real part of $E^K(\epsilon)$ is approximately $K+\frac{1}{2}$ while the imaginary part is very small. Thus, to prevent $\mathrm{Im}E^K(\epsilon)$ from being eclipsed, it is necessary to separate Eq. (3.2) into its real and imaginary parts. For this purpose we let

$$E^K(\epsilon)=E_1^K(\epsilon)+iE_2^K(\epsilon)$$
$$\sim K+\tfrac{1}{2}+iE_2^K(\epsilon), \tag{3.5a}$$

$$\Phi(x)=\Phi_1(x)+i\Phi_2(x). \tag{3.5b}$$

Furthermore, for sufficiently large x in the range $0<x<\epsilon^{-1/2}$, $\Phi(x)$ consists of an increasing and a decreasing part (see Fig. 3). We choose the phase of $\Phi(x)$, without loss of generality, such that the *decreasing part is purely real*. [We will see that the decreasing part behaves like $D_K(x)$ in regions A and B, below.] From these considerations we have

$$\left(-\frac{d^2}{dx^2}+\frac{x^2}{4}-\epsilon\frac{x^4}{4}-K-\frac{1}{2}\right)\Phi_1(x)=0 \tag{3.6a}$$

and

$$\left(\frac{d^2}{dx^2}+\frac{x^2}{4}-\epsilon\frac{x^4}{4}-K-\frac{1}{2}\right)\Phi_2(x)=E_2\Phi_1(x). \tag{3.6b}$$

In Eq. (3.6a) we have neglected $E_2\Phi_2$ compared with $E_1\Phi_1$ (see Fig. 3).

Our procedure will be to solve for Φ_1 approximately using Eq. (3.6a) and then to use this result to solve Eq. (3.6b) for Φ_2 and ultimately E_2. Our approximation scheme is based on dividing the x axis into four regions (see Fig. 3): region A, where $x\gtrsim(4K+2)^{1/2}=O(1)$; region B, where $x\gg(4K+2)^{1/2}$ but $x\ll\epsilon^{-1/2}$; region C, where $x\lesssim\epsilon^{-1/2}$; region D, where $x\sim\epsilon^{-1/2}$.

A. Φ_1 in Region A

In region A, we approximate Eq. (3.6a) by

$$\left(-\frac{d^2}{dx^2}+\frac{x^2}{4}-K-\frac{1}{2}\right)\Phi_{1A}=0, \tag{3.7}$$

to lowest order in ϵ. The solution to Eq. (3.7) which decreases for increasing x (see Fig. 3) is[16]

$$\Phi_{1A}=D_K(x), \tag{3.8}$$

where we have chosen the normalization of Φ_{1A} without loss of generality. Note that[16]

$$D_K(x)=2^{-K/2}e^{-x^2/4}H_K(x/\sqrt{2}) \tag{3.9}$$

satisfies Eq. (3.3). When x is large[16] (x approaches region B)

$$\Phi_{1A}\sim x^K e^{-x^2/4}. \tag{3.10}$$

B. Φ_2 in Region B

In regions B and C we approximate Φ_1 using lowest-order WKB:

$$\Phi_{1\,\mathrm{WKB}}=C_1(x^2-\epsilon x^4-4K-2)^{-1/4}$$
$$\times\exp\left(-\tfrac{1}{2}\int_{x_0}^{x}(t^2-\epsilon t^4-4K-2)^{1/2}\,dt\right), \tag{3.11}$$

where

$$x_0=(4K+2)^{1/2}. \tag{3.12}$$

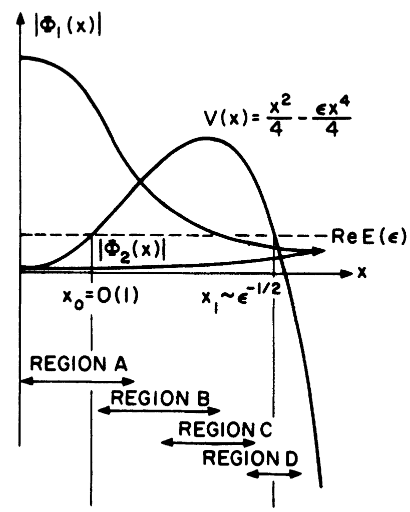

FIG. 3. Relative sizes of $|\Phi_1(x)|$ and $|\Phi_2(x)|$, which are exponentially decreasing and increasing functions of x. Regions A, B, C, and D and turning points at $x=x_0$ and $x=x_1$ are indicated.

In Eq. (3.11) we have only taken the *decreasing* exponential term (see Fig. 3). We will use the increasing exponential when we approximate Φ_2.

When x is near region B, we perform the integral in Eq. (3.11) approximately and get

$$\Phi_{1B} \sim C_1 e^{-x^2/4} x^K \exp\{\tfrac{1}{2}(K+\tfrac{1}{2})[1-\ln(K+\tfrac{1}{2})]\}. \tag{3.13}$$

Comparing Eqs. (3.10) and (3.13) gives

$$C_1 = \exp\{\tfrac{1}{2}(K+\tfrac{1}{2})[\ln(K+\tfrac{1}{2})-1]\}. \tag{3.14}$$

C. Φ_1 in Region C

When x is near the distant turning point at x_1,

$$x_1 \sim \frac{1}{\sqrt{\epsilon}}, \tag{3.15}$$

Equation (3.11) gives[17]

$$\Phi_{1C}(x) \sim (2x_1 - 2x)^{-1/4}\epsilon^{1/8} \times \exp[\tfrac{1}{3}\sqrt{2}\,\epsilon^{-1/4}(x_1-x)^{3/2} - 1/6\epsilon - (\tfrac{1}{2}K+\tfrac{1}{4})\ln(\tfrac{1}{4}\epsilon)], \tag{3.16}$$

where we have used Eq. (3.14).

D. Φ_1 and Φ_2 in Region D

In region D we substitute

$$r = (x_1 - x)(2\sqrt{\epsilon})^{-1/3}$$

into Eq. (3.2). Note that in region D we treat Φ_1 and Φ_2 at the same time – they are the same order of magnitude (see Fig. 3). In terms of r, Eq. (3.2) is approximately

$$\left(\frac{d^2}{dr^2} - r\right)\Phi_D(r) = 0, \tag{3.17}$$

which is the Airy equation.[18] Two linearly independent solutions to Eq. (3.17) are $\mathrm{Ai}(r)$ and $\mathrm{Bi}(r)$. Thus,

$$\Phi_D(x) = D_1\,\mathrm{Ai}(r) + D_2\,\mathrm{Bi}(r). \tag{3.18}$$

When we allow $x \to +\infty$, that is, $r \to -\infty$, we consult the formulas[19]

$$\mathrm{Ai}(-\rho) \sim \pi^{-1/2}\rho^{-1/4}\sin(\tfrac{2}{3}\rho^{3/2}+\tfrac{1}{4}\pi), \tag{3.19a}$$

$$\mathrm{Bi}(-\rho) \sim \pi^{-1/2}\rho^{-1/4}\cos(\tfrac{2}{3}\rho^{3/2}+\tfrac{1}{4}\pi), \tag{3.19b}$$

as $\rho \to +\infty$. However, Φ_D must have only decreasing phase as $x \to \infty$ [Eq. (3.4)]. From this requirement we obtain

$$D_1 = -iD_2 \equiv -iD. \tag{3.20}$$

Thus,

$$\Phi_D(x) = D[-i\,\mathrm{Ai}(r) + \mathrm{Bi}(r)]. \tag{3.21}$$

When $x \to 0$, $r \to +\infty$, and we consult the formulas[20]

$$\mathrm{Ai}(\rho) \sim \tfrac{1}{2}\pi^{-1/2}\rho^{-1/4}\exp(-\tfrac{2}{3}\rho^{3/2}), \tag{3.22a}$$

$$\mathrm{Bi}(\rho) \sim \pi^{-1/2}\rho^{-1/4}\exp(\tfrac{2}{3}\rho^{3/2}), \tag{3.22b}$$

as $\rho \to +\infty$. Recall that Φ_1, the real part of Φ, is decreasing as $x: 0 \to x_1$. We thus take D real and identify the decreasing and increasing solutions with the real and imaginary solutions:

$$\Phi_{1D}(x) = D\,\mathrm{Bi}(r), \tag{3.23a}$$

$$\Phi_{2D}(x) = D\,\mathrm{Ai}(r). \tag{3.23b}$$

Moreover, Eqs. (3.23a), (3.22b), and (3.16) enable us to match Φ_{1C} and Φ_{1D} asymptotically and thus to determine that

$$D = \epsilon^{1/12}\pi^{1/2}2^{-1/3}\exp[-1/6\epsilon - \tfrac{1}{2}(K+\tfrac{1}{2})\ln(\tfrac{1}{4}\epsilon)]. \tag{3.24}$$

Now that D is known, we easily calculate the asymptotic behavior of Φ_2 in region D for large r (that is, for $x < x_1$):

$$\Phi_{2D} \sim -\epsilon^{1/8}2^{-5/4}(x_1-x)^{-1/4} \times \exp[-\tfrac{1}{3}\sqrt{2}\,\epsilon^{-1/4}(x_1-x)^{3/2} - 1/6\epsilon - (\tfrac{1}{2}K+\tfrac{1}{4})\ln(\tfrac{1}{4}\epsilon)]. \tag{3.25}$$

E. Φ_2 in Region C

In regions B and C we neglect $E_2\Phi_1$ compared with $E_1\Phi_2$ in Eq. (3.6b). Thus, the WKB approximation to Φ_2 that applies in these regions is the same as that given for Φ_2 in Eq. (3.11). However, we choose a new constant C_2 and change the sign in the exponential because Φ_2 is an increasing function (see Fig. 3):

$$\Phi_{2\mathrm{WKB}} = C_2(x^2 - \epsilon x^4 - 4K - 2)^{-1/4}\exp\left(\tfrac{1}{2}\int_{x_0}^{x}(t^2 - \epsilon t^4 - 4K - 2)\,dt\right). \tag{3.26}$$

In region C, we approximate Eq. (3.26) by

$$\Phi_{2C} \sim C_2\epsilon^{1/8}(2x_1-2x)^{-1/4}\exp\{-\tfrac{1}{3}\sqrt{2}\,\epsilon^{-1/4}(x_1-x)^{3/2} + 1/6\epsilon - (\tfrac{1}{2}K+\tfrac{1}{4})[1-\ln(\tfrac{1}{4}\epsilon) - \ln(K+\tfrac{1}{2})]\}. \tag{3.27}$$

Comparing this result with Eq. (3.25) gives

$$C_2 = -\tfrac{1}{2}e^{-1/3\epsilon}\exp\{-(K+\tfrac{1}{2})[\ln(\tfrac{1}{4}\epsilon) - \tfrac{1}{2} + \tfrac{1}{2}\ln(K+\tfrac{1}{2})]\}. \tag{3.28}$$

F. Φ_2 in Region B

Now that C_2 is known, we use Eq. (3.26) again to determine the asymptotic behavior of Φ_2 in region B. We find that

$$\Phi_{2B} \sim -\tfrac{1}{2} e^{-1/3\epsilon} e^{-(K+1/2)\ln(\epsilon/4)+x^2/4} x^{-K-1} . \quad (3.29)$$

G. Φ_2 in Region A

In region A, we must not neglect $E_2\Phi_1$ compared with $E_1\Phi_2$. However, we do neglect $\frac{1}{4}\epsilon x^4$ compared with $\frac{1}{4}x^2$. Thus, we must solve the differential equation

$$(-d^2/dx^2 + \tfrac{1}{4}x^2 - K - \tfrac{1}{2})\Phi_{2A}(x) = E_2\Phi_{1A}(x) , \quad (3.30)$$

for the eigenvalue E_2. The boundary conditions on Φ_{2A} at $x=0$ are those given in Eq. (3.3). The large-x behavior of Φ_{2A} is given in Eq. (3.29).

To solve Eq. (3.30) we reduce it to a homogeneous equation as follows: Recall that E_2 is very small, and that Φ_{2A} is exponentially small compared to Φ_1 in region A. Then consider a perturbation expansion in powers of E_1 of the form

$$\Phi(x) = \Phi_{1A} + E_2\left(\frac{\Phi_{2A}}{E_2}\right) + \cdots . \quad (3.31)$$

$\phi(x)$ solves the equation

$$(-d^2/dx^2 - K - \tfrac{1}{2} - E_2 + \tfrac{1}{4}x^2)\phi(x) = 0 . \quad (3.32)$$

To verify Eq. (3.32), observe that to lowest order in E_2, it reduces to Eq. (3.7); to next order in E_2 it is precisely Eq. (3.30).

The even- (and odd-) parity solutions of Eq. (3.32) [those obeying Eq. (3.3)] are[16]

$$\phi(x) = \tfrac{1}{2}[D_{K+E_2}(x) + (-1)^K D_{K+E_2}(-x)] . \quad (3.33)$$

The factor of $\frac{1}{2}$ comes from comparing Eq. (3.33) with the result for lowest order in E_2. That is, if we let $E_2=0$ in Eq. (3.33), the expression reduces to $\phi(x)|_{E_2=0} = \Phi_{1A}(x) = D_K(x)$, which agrees with Eq. (3.9).

To next order in E_2 we get

$$\frac{\Phi_{2A}}{E_2} = \frac{1}{2}\frac{\partial}{\partial E_2}[D_{K+E_2}(x) + (-1)^K D_{K+E_2}(-x)]\bigg|_{E_2=0} . \quad (3.34)$$

E_2 will be determined by demanding that as $x\to\infty$, Eqs. (3.34) and (3.29) agree. The dominant large-x behavior of Φ_{2A}, which comes from the second term in Eq. (3.34), is[21]

$$\Phi_{2A}(x) = \left[\frac{E_2}{2}\frac{\partial}{\partial E_2}\frac{(2\pi)^{1/2}}{\Gamma(-K-E_2)} \times e^{(K+E_2)\pi i} x^{-(K+E_2+1)} e^{x^2/4}\right]\bigg|_{E_2=0} . \quad (3.35)$$

Demanding that Eqs. (3.35) and (3.29) agree to lowest order in ϵ and E_2 gives the result

$$E_2 = \frac{4^{K+1/2}}{K!\sqrt{2\pi}} e^{-1/3\epsilon} \epsilon^{-K-1/2} . \quad (3.36)$$

Equation (3.36) is the result we have sought. Note that E_2 is exponentially small, which justifies *a posteriori* our neglecting of $E_2\Phi_1$ compared with $E_1\Phi_2$ in part E of this calculation. In the next section we use Eq. (3.36) and the dispersion integral of Sec. II to determine the large-order behavior of perturbation theory. In the appendix we give a very short and intuitive derivation of Eq. (3.36).

IV. LOWEST-ORDER WKB RESULTS

In this section we show how to use Eq. (3.36), the result of the lowest-order WKB calculation, to obtain the dominant large-n behavior of the Rayleigh-Schrödinger coefficients.

First, we compute $D^K(x)$ by combining Eqs. (2.1) and (2.6) with (3.6). We find that to lowest order in x (x is small and negative)

$$D^K(x) = -\frac{4^{K+1}i}{K!(2\pi)^{1/2}} e^{1/3x}(-x)^{-K-3/2} . \quad (4.1)$$

To compute the discontinuity D in Eq. (4.1), it is necessary to use a well-known property of $E^K(\lambda)$, namely,[2]

$$E^K(\lambda) = E^{K*}(\lambda^*) . \quad (4.2)$$

Next we substitute Eq. (4.1) into Eq. (2.7) and obtain for large n

$$A_n^K = \frac{-4^K\sqrt{2}}{K!\pi^{3/2}}\int_{-\infty}^0 dx\, x^{-n} e^{1/3x}(-x)^{-K-3/2} . \quad (4.3)$$

Performing the integral in Eq. (4.3) exactly gives the leading large-n behavior of A_n (see Ref. 22):

$$A_n^K = \frac{(-1)^{n+1}12^K\sqrt{6}}{K!\pi^{3/2}} 3^n\,\Gamma(n+K+\tfrac{1}{2})[1+O(1/n)] . \quad (4.4)$$

We have indicated that the corrections to Eq. (4.4) are of order n^{-1}. This is verified in the next section, where we derive the next-higher-order WKB results. We emphasize here that *lowest-order WKB is sufficient to give the precise leading behavior of A_n^K for large n.* Successively higher-order WKB approximations to $\mathrm{Im}E^K(\lambda)$ do not change the results in Eq. (4.4); rather, they give the successive coefficients of inverse powers of n which multiply the leading behavior in Eq. (4.4). Equation (4.4) is the first term of a series in powers of n^{-1} (which may be asymptotic).

V. FIRST-ORDER WKB RESULTS

In this section we obtain the $O(n^{-1})$ corrections to Eq. (4.4). We could, of course, accomplish this task by carrying out the WKB calculations of Sec. III to order ϵ, plugging those results into Eq. (2.7), and evaluating the integral. Instead of presenting this extremely tedious and unenlightening calculation, we will rely on previous WKB calculations,[2] and, with a minimum of work, determine the $O(n^{-1})$ corrections. Our procedure will be to (A) compare the results of Sec. III with previous zeroth-order WKB calculations, and (B) use this comparison to find the first-order WKB result corresponding to Eq. (3.36).

A. Discussion of Zeroth-Order WKB

In Ref. 2 the approximate λ dependence of the energy levels $E^K(\lambda)$ was discovered through the use of WKB techniques. When $|\lambda|$ is small and $|\arg\lambda| < \pi$,

$$E^K(\lambda) = K + \tfrac{1}{2} + O(\lambda). \tag{5.1}$$

Thus, as $\arg\lambda$ increases from 0 to π, the energy eigenvalues stay very near the points $K+\frac{1}{2}$ on the positive real axis. As $\arg\lambda$ increases from π to $3\pi/2$, the eigenvalues move abruptly to the ImE axis. These trajectories in the complex E plane are governed by[2]

$$\frac{\Gamma(\frac{1}{4}+\frac{1}{2}E^K)}{\Gamma(\frac{1}{4}-\frac{1}{2}E^K)} = \exp\left(\frac{1}{3\lambda} + \frac{5\pi i}{4} - E^K \ln(\tfrac{1}{2} i\lambda)\right), \tag{5.2a}$$

for even-parity energy levels (K even), and

$$\frac{\Gamma(\frac{3}{4}+\frac{1}{2}E^K)}{\Gamma(\frac{3}{4}-\frac{1}{2}E^K)} = \exp\left(\frac{1}{3\lambda} - \frac{5\pi i}{4} - E^K \ln(\tfrac{1}{2} i\lambda)\right), \tag{5.2b}$$

for odd-parity energy levels.

As we emphasized in Sec. II, Eq. (5.1) is valid when $|\arg\lambda| < \pi$, and Eq. (5.2) is valid when $\pi < |\arg\lambda| \le 2\pi$. When $|\arg\lambda| = \pi$, the point at which the distant turning point enters the sector in the complex x plane where the boundary condition $\lim_{|x|\to\infty}\psi(x)=0$ holds, we have from Sec. III

$$\operatorname{Re} E^K(\lambda) = K + \tfrac{1}{2} + O(\lambda) \tag{5.3a}$$

and

$$\operatorname{Im} E^K(\lambda) = \pm \frac{4^{K+1/2}}{K!(2\pi)^{1/2}} e^{1/3\lambda}(-\lambda)^{-K-1/2}[1+O(\lambda)], \tag{5.3b}$$

where the $\pm$ corresponds to $\arg\lambda = \pm\pi$.

We raise the following question: What do we get from Eqs. (5.1) and (5.2) if they are assumed to be valid at $\arg\lambda = \pm\pi$? For this purpose, we must consider the real part and the imaginary part of $E^K(\lambda)$ separately because, as seen from Eq. (5.3), for $|\arg\lambda| = \pi$, the imaginary part is exponentially small compared with the real part. Consider the real part first. Equation (5.3a) agrees trivially with Eq. (5.1) for $|\arg\lambda| = \pi$. Furthermore, for $\arg\lambda = \pi$, the right-hand sides of Eqs. (5.2a) and (5.2b) are exponentially small and hence may be neglected. Accordingly, we get Eq. (5.3a) once again from Eqs. (5.2a) and (5.2b).

It is much more interesting to compare the imaginary parts. If Eq. (5.1) is assumed to hold for $|\arg\lambda| = \pi$, then, since the coefficient of every power of λ is real, we must conclude that

$$\operatorname{Im} E^K(\lambda) = 0. \tag{5.4}$$

More care must be taken with Eq. (5.2). Consider first the even-parity energy levels,

$$\begin{aligned} E^K &= E^{2J} \\ &= 2J + \tfrac{1}{2} + iE_2, \end{aligned} \tag{5.5}$$

where E_2 is assumed to be exponentially small (of order $e^{1/\lambda}$, for λ negative real). We approximate the left-hand side of Eq. (5.2a) as follows[23]:

$$\begin{aligned} \frac{\Gamma(\frac{1}{4}+\frac{1}{2}E^K)}{\Gamma(\frac{1}{4}-\frac{1}{2}E^K)} &\sim \frac{\Gamma(J+\frac{1}{2})}{\Gamma(-J-iE_2/2)} \\ &\sim \frac{\Gamma(J+\frac{1}{2})\Gamma(J+1)\sin(\pi J + \pi i E_2/2)}{-\pi} \\ &\sim i\sqrt{\pi}\, 2^{-2J-1} E_2 (-1)^{J+1}(2J)!\,. \end{aligned} \tag{5.6}$$

The right-hand side of Eq. (5.2a) is approximately

$$\begin{aligned} &e^{1/3\lambda} e^{5\pi i/4}(-\tfrac{1}{2}\lambda)^{-E^K} e^{-E^K \ln(-i)} \\ &\quad\sim i e^{1/3\lambda} e^{5\pi i/4}(-\tfrac{1}{2}\lambda)^{-2J-1/2} e^{(2J+1/2)\ln i} \\ &\quad\sim e^{1/3\lambda}(-1)^{J+1}(-\tfrac{1}{2}\lambda)^{-2J-1/2}, \end{aligned} \tag{5.7}$$

where we have chosen that branch of the ln function for which $\ln i = \frac{1}{2} i\pi$. Combining Eqs. (5.6) and (5.7) gives

$$E_2 \sim \frac{\sqrt{2}\, 4^{2J+1/2}}{\sqrt{\pi}(2J)!} e^{1/3\lambda}(-\lambda)^{-2J-1/2}. \tag{5.8}$$

By an analogous procedure, we have

$$E_2 \sim \frac{\sqrt{2}\, 4^{2J+3/2}}{\sqrt{\pi}(2J+1)!} e^{1/3\lambda}(-\lambda)^{-2J-3/2}, \tag{5.9}$$

for odd-parity energy levels of the form

$$\begin{aligned} E^K &= E^{2J+1} \\ &= 2J + \tfrac{3}{2} + iE_2\,. \end{aligned}$$

Equations (5.8) and (5.9) verify the assumption that E_2 is exponentially small.

Finally we combine Eqs. (5.8) and (5.9) into one:

$$\mathrm{Im}E^K(\lambda) \sim \frac{\sqrt{2}\, 4^{K+1/2}}{\sqrt{\pi}\, K!} e^{1/3\lambda}(-\lambda)^{-K-1/2}. \tag{5.10}$$

Again we observe a disagreement with Eq. (5.3b) – the imaginary part of the energy in Eq. (5.10) is too large by a factor of 2. Specifically, this factor arises from the equations for the asymptotic behavior of the Airy functions [see Eqs. (3.19) and (3.22)]. However, factors of 2 appear quite generally in Stokes' related discontinuous phenomena. In our case the discontinuity occurs when the distant turning point crosses a Stokes line of the asymptotic expansion of $\psi(x)$ for large x. The Stokes line is the edge of the sector in which $\psi(x) \to 0$ for large x.

A simple example illustrating this discontinuous phenomenon is a contour integral in the complex plane where the contour is shifted so that it passes through a simple pole. When the pole lies on the contour there is a discontinuity in the value of the integral which may be obtained by the principal-parts method. If we average the integrals for the pole lying inside and outside the contour, we obtain the principal-parts result.

Keeping these comments in mind, we are now not surprised to observe that Eq. (5.3b) is precisely the average of Eqs. (5.4) and (5.10). This averaging phenomenon is quite general. We will use it in Sec. V B to determine $E^K(\lambda)$, $\lambda<0$, to first order in λ by averaging the first-order versions of Eqs. (5.4) and (5.10).

Finally, we point out one further way of understanding this averaging. With reference to Sec. II, suppose we take the cut not along the $\arg\lambda = 180°$ direction, but at $\arg\lambda = 179°$. Then the discontinuity is given by

$$E^K(\arg\lambda = 179°) - E^K(\arg\lambda = -181°).$$

The first term can be computed from Eq. (5.1) and the second from Eq. (5.2). Some contributions such as $K+\frac{1}{2}$ cancel and we get the sum of Eqs. (5.4) and (5.10) after analytically continuing the discontinuity to 180°.

B. First-Order WKB Results

The first-order analog of Eq. (5.1) is

$$E^K(\lambda) = K + \tfrac{1}{2} + \tfrac{3}{4}(2K^2 + 2K + 1)\lambda + O(\lambda^2). \tag{5.11}$$

Equation (5.11) follows from a straightforward application of Rayleigh-Schrödinger perturbation theory to Eqs. (1.1) and (1.2). The first-order analog of Eq. (5.2a) is[24]

$$\frac{\Gamma(\frac{1}{2}+\frac{1}{2}\nu)}{\Gamma(-\frac{1}{2}\nu)} = \exp\left(\frac{1}{3\lambda} + \frac{5\pi i}{4} - (\nu+\tfrac{1}{2})\ln(\tfrac{1}{2}i\lambda) + \lambda A + \lambda B E^2\right), \tag{5.12}$$

where

$$\nu \equiv E - \tfrac{1}{2} - 3\lambda(E^2 + \tfrac{1}{4})/2. \tag{5.13}$$

The values of A and B in Ref. 2 are incorrect. Their correct values are

$$A = \tfrac{67}{48}, \quad B = \tfrac{17}{4}. \tag{5.14}$$

Equations (5.13) and (5.1) imply that for the Jth even-parity energy level,

$$\nu = 2J + \eta, \tag{5.15}$$

where η is at most of order λ. We insert this result into Eq. (5.12) and find that (as in Sec. V A) the left-hand side reduces to η times a constant while the right-hand side is of order $e^{1/3\lambda}$. Thus, for negative real λ, *η is smaller than any power of λ.* Noting this result, we return to Eq. (5.13) and iterate it once to get an approximate expression for $E^K(\lambda) = E^{2J}(\lambda)$:

$$E^{2J} = 2J + \tfrac{1}{2} + \tfrac{3}{4}\lambda(8J^2 + 4J + 1) + \eta[1 + \tfrac{3}{2}\lambda(1+4J)]. \tag{5.16}$$

Equation (5.16), the first-order version of Eq. (5.4), contains λ twice. Apparently, the real and the imaginary parts of E (η is imaginary, as will be seen shortly) express their higher-order corrections in separate and independent power series in λ.

Next, we use Eqs. (5.12), (5.15), and (5.16) to evaluate η. The left-hand side of Eq. (5.12) reduces to

$$\sqrt{\pi}\, 2^{-2J-1}(-1)^{J+1}(2J)!\,\eta, \tag{5.17}$$

following the procedure of Eq. (5.5). The right-hand side of Eq. (5.12) is approximated by

$$e^{1/3\lambda} e^{5\pi i/4}[1+\lambda(A+BE^2)]\, e^{-(2J+1/2)\ln(i\lambda/2)} \sim e^{1/3\lambda} i[1+\lambda(A+BE^2)](-\tfrac{1}{2}\lambda)^{-2J-1/2}(-1)^{J+1}. \tag{5.18}$$

Combining Eqs. (5.17) and (5.18) gives

$$\eta = \frac{i\sqrt{2}\, 4^{2J+1/2}}{\sqrt{\pi}\,(2J)!} e^{1/3\lambda}(-\lambda)^{-2J-1/2}[1+\lambda(A+BE^2)]. \tag{5.19}$$

Next, we combine Eq. (5.19) with (5.16):

$$E^{2J} = 2J + \tfrac{1}{2} + \tfrac{3}{4}\lambda(8J^2 + 4J + 1) + \frac{i\sqrt{2}\,4^{2J+1/2}}{\sqrt{\pi}\,(2J)!}\, e^{1/3\lambda}(-\lambda)^{-2J-1/2}\{1 + \lambda[\tfrac{3}{2} + 6J + A + B(2J + \tfrac{1}{2})^2]\}. \tag{5.20}$$

Finally, we replace $2J$ in Eq. (5.20) with K and have for all energy levels

$$E^{K} = K + \tfrac{1}{2} + \tfrac{3}{4}\lambda(2K^2 + 2K + 1) + \frac{i\sqrt{2}\,4^{K+1/2}}{\sqrt{\pi}\,K!}\, e^{1/3\lambda}(-\lambda)^{-K-1/2}\{1 + \lambda[\tfrac{3}{2} + 3K - A - B(K + \tfrac{1}{2})^2]\}. \tag{5.21}$$

The imaginary part of Eq. (5.21) is the first-order generalization of Eq. (5.10). Note that the real parts of Eqs. (5.21) and (5.11) are identical and that only Eq. (5.21) has a nonzero imaginary part (as was true of the zeroth-order counterparts of these equations).

As in Sec. V A we can now *average* the expressions in Eqs. (5.11) and (5.21) to obtain the true value of $E^K(\lambda)$ for $\lambda < 0$. This true value differs from Eq. (5.21) in that the $\sqrt{2}$ is in the denominator. From this result we obtain the discontinuity which was defined in Eq. (2.6):

$$D^K(x) = -\frac{4^{K+1}i}{K!\,(2\pi)^{1/2}}\, e^{1/3x}(-x)^{-K-3/2} \times [1 + x(\tfrac{95}{24} + \tfrac{29}{4}K + \tfrac{17}{4}K^2)], \tag{5.22}$$

where we have substituted the values of A and B given in Eq. (5.14).

We can now compute the $O(n^{-1})$ corrections to Eq. (4.4). Following the procedure of Sec. IV, we insert Eq. (5.22) into Eq. (2.7), perform the integral, and obtain for large n

$$A_n^K = \frac{(-1)^{n+1}12^K\sqrt{6}}{K!\,\pi^{3/2}}\, 3^n\Gamma(n + K + \tfrac{1}{2}) \times\left(1 - \frac{1}{n}(\tfrac{95}{72} + \tfrac{29}{12}K + \tfrac{17}{12}K^2) + O(n^{-2})\right). \tag{5.23}$$

This is the desired result which was stated in Sec. I. It is a generalization to all K of Eq. (4) in Ref. 1.

We conclude with two remarks. First, recall that in Ref. 2 there is a numerical fit of the first 75 Rayleigh-Schrödinger coefficients for the ground-state energy ($K = 0$).[25] There, the coefficient of n^{-1} is given as

$$-1.319\,453\,.$$

The decimal equivalent of $-\frac{95}{72}$, the exact answer in Eq. (5.23), is

$$-1.319\,444\cdots.$$

This agreement strongly testifies to the power of WKB analysis.

Second, recall that as pointed out in Sec. IV, A_n^K will in general be given by the result in Eq. (4.4) [and Eq. (5.23)] followed by a series in inverse powers of n. [This must be so because the corrections to the discontinuity $D^K(x)$, in Eq. (5.22), for example, are a power series in x.] The series for A_n^0 will thus take the form

$$A_n^0 \sim (-1)^{n+1}\frac{\sqrt{6}}{\pi^{3/2}}\Gamma(n + \tfrac{1}{2})3^n\left(1 - \sum_{j=1}^{\infty}\frac{a_j}{n^j}\right). \tag{5.24}$$

We would not be surprised if the series in Eq. (5.24) is asymptotic. In fact, we would not even be surprised to find that the coefficients a_j are all positive, rational fractions. We have calculated numerically some of the coefficients a_j and have obtained the following results[26]:

$$a_1 = \tfrac{95}{72},$$

$$a_2 = \tfrac{20\,099}{10\,368}\ (= 1.938\,560\,9_{567\,901\,234}),$$

$$a_3 = \tfrac{15\,422\,651}{2\,198\,748}.$$

These values for a_1, a_2, and a_3 were of course originally computed as decimals; afterward, we guessed the above fractional representations of which we are extremely confident. Note that the denominators are all products of powers of 2 and 3.

We have also computed these additional coefficients:

$$a_4 = 40.118\,943\,1\,,$$

$$a_5 = 305.5223\,,$$

$$a_6 = 2808.09\,,$$

$$a_7 = 0.2995\times10^5\,,$$

$$a_8 = 0.365\times10^6\,,$$

$$a_9 = 0.44\times10^7\,,$$

$$a_{10} = 1\times10^8\,.$$

It is not yet possible to determine the fractional representations for the above coefficients because they are not known to a sufficient number of significant figures.

VI. INDEPENDENT DERIVATION

We exhibit below a new and independent derivation of Eq. (4.4) for the ground-state ($K = 0$) energy. At the end of this section, we generalize these results to the first energy level. Our methods here are far more direct, although somewhat more involved, than those of Secs. II, III, and IV. We will find a *linear* difference equation which for large n asymptotically approximates the nonlinear difference equation [Eq. (6.3)] which generates nth-order perturbation theory. We then solve this linear difference equation. Our methods are nonrigorous; nonetheless, we feel that this analysis is extremely worthwhile because it clarifies the rather subtle and intricate perturbative structure of the anharmonic oscillator model.

We obtain the nonlinear difference equation which generates the ground-state energy perturbation series by substituting

$$E^0(\lambda) \sim \tfrac{1}{2} - \sum_{n=1}^{\infty} (-\lambda)^n C_n \tag{6.1}$$

and

$$\psi^0(x) \sim e^{-x^2/4}\left(1 + \sum_{n=1}^{\infty} (-\lambda)^n \sum_{j=1}^{2n} (\tfrac{1}{2}x^2)^j C_{n,j}\right) \tag{6.2}$$

into the differential equation in Eq. (1.1). Collecting powers of x and λ gives the desired difference equation[27]:

$$2jC_{n,j} = (j+1)(2j+1)C_{n,j+1} + C_{n-1,j-2} - \sum_{p=1}^{n-1} C_{p,1}C_{n-p,j}\,, \tag{6.3}$$

where $C_n = C_{n,1}$ and $C_{0,0} = 1$. The C_n are related to the Rayleigh-Schrödinger coefficients A_n^0 by the formula

$$A_n^0 = (-1)^{n+1}C_n\,. \tag{6.4}$$

The minus signs in Eqs. (6.1) and (6.2) are chosen so that the $C_{n,j}$ are all positive.

Figure 4 illustrates schematically how Eq. (6.3) iterates. The dots represent the nonzero entries in the matrix $C_{n,j}$. The dot in the circle represents the value of $C_{n,j}$ to be computed, that is, the left-hand side of Eq. (6.3). The underlined dots are the values of $C_{n,j}$ on the right-hand side of Eq. (6.3).

A glance at Fig. 4 indicates several general properties of Eq. (6.3). Each $C_{n,j}$ depends on all numbers above and to the right of it. Thus, the matrix in Fig. 4 must be filled out from right to left for fixed n; after each row is completed, n, the order of perturbation theory, is increased by unity. As is typical in perturbation theory, each new order is increasingly difficult to compute because it depends on *all* previous orders. Note, however, that it is easy to find exact formulas for the entries on the right-hand side of the matrix:

$$C_{n,2n} = \frac{1}{4^n n!}\,, \tag{6.5a}$$

$$C_{n,2n-1} = \frac{4n+5}{3\,4^n(n-1)!}\,, \tag{6.5b}$$

$$C_{n,2n-2} = \frac{16n^2+64n+87}{18\,4^n(n-2)!}\,. \tag{6.5c}$$

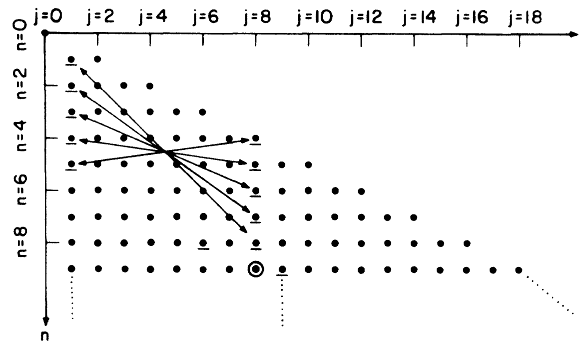

FIG. 4. Schematic representation of Eq. (6.3). The dots represent the nonzero values of $C_{n,j}$. The dot in the circle is the value of $C_{n,j}$ to be computed; the underlined dots are the values of $C_{n,j}$ which Eq. (6.3) requires for this computation. The arrows indicate those pairs of $C_{n,j}$ which are multiplied together.

Our problem is to find the large-n behavior of $C_{n,1}$, the entries in the first column of the matrix.

A. Linearization of Eq. (6.3)

The positivity of $C_{n,j}$ implies that the summation on the right-hand side of Eq. (6.3) is small compared with the other two terms. This suggests that Eq. (6.3) may be replaced by a sequence of *linear* equations, the Nth equation having the summation in

$$-\sum_{p=1}^{n-1} C_{p,1}C_{n-p,j}$$

replaced by $\sum_{p=1}^{N}$ and $\sum_{p=n-N}^{n-1}$, where $N=0$ means no sum is performed, and where the actual numerical values of $C_{p,j}$, $1 \leq p \leq N$ are calculated and then inserted into the summation. One would expect that as N increases one obtains a better approximation to $C_{n,1}$. This has been verified to order 150 on a computer where we found that

$$C_{n,1}/C_{n,1}(N=0) \sim 1 + O(1/n)\,,$$

$$C_{n,1}/C_{n,1}(N=1) \sim 1 + O(1/n^2)\,,$$

$$C_{n,1}/C_{n,1}(N=2) \sim 1 + O(1/n^3)\,, \quad \text{etc.}$$

We now demonstrate analytically that the $N=0$ linear equation

$$2jC_{n,j} = (j+1)(2j+1)C_{n,j+1} + C_{n-1,j-2}\,, \quad C_{0,0} = 1 \tag{6.6}$$

gives the same leading behavior of $C_{n,1}$ for large n as in Eq. (4.4). The $N \geq 1$ equations have still not been solved analytically.

B. Approximation of the Linear Equation

Equation (6.6) may be further approximated. Detailed inspection of computer output shows that for large n,

$$(j+1)(2j+1)C_{n,j+1} \gg C_{n-1,j-2}, \quad \text{for } j=O(1) \tag{6.7a}$$

$$(j+1)(2j+1)C_{n,j+1} \ll C_{n-1,j-2}, \quad \text{for } j=O(2n). \tag{6.7b}$$

Equation (6.6) suggests the substitution

$$D_{n,j}=j\Gamma(j+\tfrac{1}{2})C_{n,j}, \tag{6.8}$$

which gives

$$D_{n,j}=D_{n,j+1}+\left(\frac{j}{2}+\frac{3}{8j-16}\right)D_{n-1,j-2}. \tag{6.9}$$

For large n, the term $3(8j-16)^{-1}$ can be dropped because for large j it is small compared with $\frac{1}{2}j$ and for small j Eq. (6.7a) shows that contribution from the $D_{n-1,j-2}$ term is negligible. Thus, we approximate Eq. (6.9) by

$$E_{n,j}=E_{n,j+1}+\tfrac{1}{2}jE_{n-1,j-2}. \tag{6.10}$$

However, this approximation is only good for large n. Furthermore, Eq. (6.10) is homogeneous (multiples of solutions are solutions). Therefore, we calculate the initial value $E_{0,0}$ by demanding that $E_{n,j}$ approximate $D_{n,j}$ for large n. It is simplest to require that

$$\lim_{n\to\infty}\frac{E_{n,2n}}{D_{n,2n}}=1. \tag{6.11}$$

$D_{n,2n}$ is obtained from Eqs. (6.5a) and (6.8). It is easy to see that $E_{n,2n}=E_{0,0}n!$. Thus,

$$E_{0,0}=\lim_{n\to\infty}\frac{2n\Gamma(2n+\frac{1}{2})}{4^n(n!)^2}=(2/\pi)^{1/2}. \tag{6.12}$$

Having established Eq. (6.12), we expect that for large n,

$$C_{n,1}=\frac{D_{n,1}}{\Gamma(\frac{3}{2})}=\frac{2}{\sqrt{\pi}}D_{n,1}\sim\frac{2}{\sqrt{\pi}}E_{n,1}. \tag{6.13}$$

Finally, for convenience we define a new function $F_{n,j}$ which is a multiple of $E_{n,j}$ and obeys the equations

$$F_{0,0}=1, \tag{6.14a}$$

$$F_{n,j}=F_{n,j+1}+\tfrac{1}{2}jF_{n-1,j-2}, \tag{6.14b}$$

$$C_{n,1}\sim\frac{2\sqrt{2}}{\pi}F_{n,1}. \tag{6.14c}$$

C. Conversion to a Partial Differential Equation

To solve Eq. (6.14) we define the generating functions

$$F(x)=\sum_{n=1}^{\infty}\frac{F_{n,1}x^{n-1}}{(n-1)!}, \tag{6.15a}$$

$$G(x,y)=\sum_{n=1}^{\infty}\frac{x^n}{n!}\sum_{j=1}^{2n}y^{j+2}F_{n,j}, \tag{6.15b}$$

where

$$G(x,0)=G(0,y)=0. \tag{6.16}$$

Then we multiply Eq. (6.14b) by y^{j+2} and sum over j, multiply by $x^{n-1}/(n-1)!$ and sum over n, and use Eq. (6.15) to convert the result into the partial differential equation

$$\frac{\partial}{\partial x}G(x,y)+\frac{y^4}{2(1-y)}\frac{\partial}{\partial y}G(x,y)=\frac{y^3}{y-1}[y^2-F(x)]. \tag{6.17}$$

Note that unknowns appear on *both* sides of this equation

To solve Eq. (6.17) we introduce a new variable ξ, where

$$\frac{dy}{d\xi}=\frac{y^4}{2(1-y)}. \tag{6.18}$$

Integrating Eq. (6.18) gives

$$\xi(y)=\frac{3y-2}{3y^3}. \tag{6.19}$$

$\xi(y)$ is plotted on Fig. 5. Note that for $\xi>0$, $\xi(y)$ has a two-valued inverse. The inverse functions $g_1(\xi)$ and $g_2(\xi)$ are plotted on Fig. 6. In terms of x and ξ the solution of Eq. (6.17) is

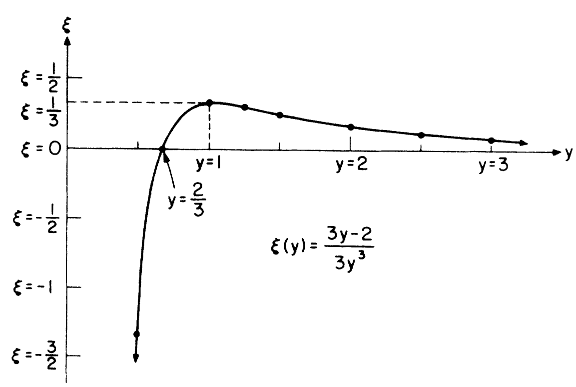

FIG. 5. Graph of $\xi(y)=(3y-2)/3y^3$ showing the two-valued inverse of $\xi(y)$ for $\xi>0$.

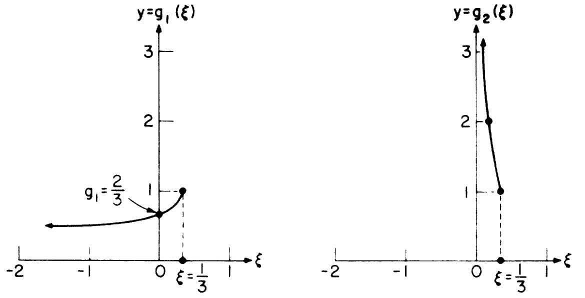

FIG. 6. Graph of the two inverse functions $y = g_1(\xi)$ and $y = g_2(\xi)$ which solve the equation $\xi(y) = (3y-2)/3y^3$.

$$G_{1,2}(x,\xi) = \int_0^x dx' \frac{g_{1,2}{}^3(\xi - x + x')}{1 - g_{1,2}(\xi - x + x')} \times [F(x') - g_{1,2}{}^2(\xi - x + x')], \quad (6.20)$$

where

$$G_{1,2}(x,\xi) = G(x, g_{1,2}(\xi)). \quad (6.21)$$

Note that Eq. (6.16) allows us to eliminate an arbitrary solution $V(x-\xi)$ of the homogeneous equation from Eq. (6.20).

The integral in Eq. (6.20) can be simplified by using Eq. (6.18) as follows:

$$-\int_0^x dx' \frac{g_{1,2}{}^5(\xi - x + x')}{1 - g_{1,2}(\xi - x + x')} = -2\int_0^x dx' g_{1,2}(\xi - x + x') \frac{dg_{1,2}(\xi - x + x')}{dx'} = -g_{1,2}{}^2(\xi) + g_{1,2}{}^2(\xi - x). \quad (6.22)$$

D. Conversion to an Integral Equation for $F(x)$

From Fig. 6 observe that $g_1(\frac{1}{3}) = g_2(\frac{1}{3})$. Hence, using Eq. (6.21), we find that

$$G_1(x, \tfrac{1}{3}) = G_2(x, \tfrac{1}{3}). \quad (6.23)$$

Combining Eqs. (6.20) and (6.23) then eliminates all reference to G and gives the following singular integral equation for F:

$$\int_0^x dx' F(x') \left[\frac{g_1{}^3(\frac{1}{3} - x + x')}{1 - g_1(\frac{1}{3} - x + x')} - \frac{g_2{}^3(\frac{1}{3} - x + x')}{1 - g_2(\frac{1}{3} - x + x')}\right] = g_2{}^2(\tfrac{1}{3} - x) - g_1{}^2(\tfrac{1}{3} - x). \quad (6.24)$$

E. Approximate Solution of the Integral Equation

Figure 6 shows that for small ξ, $g_2(\xi)$ is singular while $g_1(\xi)$ is finite. Indeed, Eq. (6.19) implies that for small ϵ,

$$g_1(\epsilon) \sim \tfrac{2}{3}, \quad (6.25a)$$

$$g_2(\epsilon) \sim \epsilon^{-1/2}. \quad (6.25b)$$

Equation (6.25) indicates that as x approaches $\frac{1}{3}$, the right-hand side of Eq. (6.24) becomes singular. We are thus motivated to identify the leading singularity in $F(x)$ which causes the equivalent divergence of the left-hand side. To this end, we substitute

$$x = \tfrac{1}{3} - \epsilon, \quad x' = \tfrac{1}{3} - \epsilon' \quad (6.26)$$

into Eq. (6.24). The resulting approximate integral equation is

$$\int_\epsilon^{1/3} d\epsilon' F(\tfrac{1}{3} - \epsilon') \left[\frac{g_1{}^3(\frac{1}{3} + \epsilon - \epsilon')}{1 - g_1(\frac{1}{3} + \epsilon - \epsilon')} - \frac{g_2{}^3(\frac{1}{3} + \epsilon - \epsilon')}{1 - g_2(\frac{1}{3} + \epsilon - \epsilon')}\right] \sim \frac{1}{\epsilon}. \quad (6.27)$$

Next we approximate the expression in square brackets in Eq. (6.27). Figure 6 shows that $g_{1,2}(\frac{1}{3}) = 1$. When ξ is near $\frac{1}{3}$ (y near unity) we can replace the differential equation in Eq. (6.18) by

$$d\xi \sim 2(1-y)dy. \quad (6.28)$$

Equation (6.28) integrates to

$$\tfrac{1}{3} - \xi = (1-y)^2. \quad (6.29)$$

Thus, using Fig. 6 to guide the choice of sign,

$$1 - g_1(\tfrac{1}{3} + \epsilon - \epsilon') \sim (\epsilon' - \epsilon)^{1/2}, \quad (6.30a)$$

$$1 - g_2(\tfrac{1}{3} + \epsilon - \epsilon') \sim -(\epsilon' - \epsilon)^{1/2}. \quad (6.30b)$$

From Eq. (6.30), we conclude that Eq. (6.27) may be further approximated by

$$\int_\epsilon^{1/3} d\epsilon' F(\tfrac{1}{3} - \epsilon') \frac{2}{(\epsilon' - \epsilon)^{1/2}} \sim \frac{1}{\epsilon}. \quad (6.31)$$

The leading singularity in F which causes the divergence of the right-hand side for small ϵ clearly has the form

$$F(\tfrac{1}{3} - \epsilon') \sim \frac{a}{\epsilon'^k}. \quad (6.32)$$

The substitution $\epsilon' = \epsilon/z$ yields $k = \frac{3}{2}$ and the equation

$$\int_{3\epsilon}^{1} \frac{dz}{(1-z)^{1/2}} = \frac{1}{2a}.$$

Letting $\epsilon \to 0$ gives $a = \frac{1}{4}$. Hence, the leading singularity of $F(x)$ is given by

$$F(x) \sim \tfrac{1}{4}(\tfrac{1}{3} - x)^{-3/2}. \quad (6.33)$$

F. Recovery of $C_{n,1}$ for Large n

The actual behavior of $F(x)$ as given by Eq. (6.24) has the form

$$F(x) \sim \tfrac{1}{4}(\tfrac{1}{3}-x)^{-3/2} + \alpha(\tfrac{1}{3}-x)^{-1/2} + \beta(\tfrac{1}{3}-x)^{1/2} + \cdots . \tag{6.34}$$

However, when $F(x)$ is expanded into a power series in x, the *dominant* contribution to the coefficient of the x^n term for large n comes from the *most* singular term in Eq. (6.34). Thus, the analysis we have carried out is just sufficient to obtain the leading behavior of C_n for large n. Hence, using the binomial theorem to get the nth term in the expansion of $\frac{1}{4}(\frac{1}{3}-x)^{-3/2}$ and combining this result with Eqs. (6.15a) and (6.14c) gives the desired result

$$C_{n,1} \sim \frac{\sqrt{6}}{\pi^{3/2}} 3^n \Gamma(n+\tfrac{1}{2}) \tag{6.35}$$

or

$$A_n^0 \sim (-1)^{n+1} \frac{\sqrt{6}}{\pi^{3/2}} 3^n \Gamma(n+\tfrac{1}{2}), \tag{6.36}$$

which agrees with the result in Eq. (4.4) when $K=0$.

G. Discussion

We discuss below one subtle aspect of this derivation. At first glance it might appear that the delicate and intricate use of the multivaluedness of y as a function of ξ to eliminate the unknown generating functions G_1 and G_2 in Sec. V D was not necessary. It would seem that a more straightforward approach would use the relation

$$F(x) \equiv 1 + \frac{1}{2} \frac{\partial G(x,y)}{\partial y}\bigg|_{y=1}. \tag{6.37}$$

This identity may be proved by differentiating G in Eq. (6.15b) and letting $y=1$. The result is

$$\begin{aligned} 1 + \frac{1}{2}\frac{\partial G}{\partial y}\bigg|_{y=1} &= 1 + \sum_{n=1}^{\infty} \frac{x^n}{n!} \sum_{j=1}^{2n} \frac{j+2}{2} F_{n,j} \\ &= 1 + \sum_{n=1}^{\infty} \frac{x^n}{n!} \sum_{j=3}^{2n+2} (F_{n+1,j} - F_{n+1,j+1}), \end{aligned} \tag{6.38}$$

where we have shifted the j index and substituted Eq. (6.14b). The j summation in Eq. (6.38) collapses. Comparing with Eq. (6.15a) verifies Eq. (6.37).

Converting the identity to one involving the x and ξ variables gives

$$F(x) \equiv 1 + \lim_{\xi \to 1/3} \left(\pm(\tfrac{1}{3}-\xi)^{1/2} \frac{\partial G_{1,2}(x,\xi)}{\partial \xi} \right). \tag{6.39}$$

It would now appear that applying Eq. (6.39) to Eq. (6.20) is a far simpler way to eliminate the unknowns $G_{1,2}$ in favor of F. In fact, this procedure leads to a tautology – the resulting equation for F reduces to an identity. The apparently new and independent condition in Eq. (6.39) is *already* contained in Eq. (6.20). Thus, we are *forced* to follow the procedure of Sec. V D.

H. First Energy Level ($K=1$)

It is easy to repeat these techniques for the first energy level. We list below some intermediate $K=1$ results, which correspond with the $K=0$ results given above.

The linearized difference equation which corresponds with Eq. (6.6) is

$$2j\, C_{n,j} = (j+1)(2j+3) C_{n,j+1} + C_{n-1,j-2}, \tag{6.40}$$

where $C_{0,0}=1$ and

$$A_n^1 = 3(-1)^{n+1} C_{n,1}. \tag{6.41}$$

To derive Eq. (6.40) we have dropped the convolution term

$$-3 \sum_{p=1}^{n-1} C_{p,j} C_{n-p,1}$$

from the right-hand side. The substitution

$$D_{n,j} = j\Gamma(j+\tfrac{3}{2}) C_{n,j}$$

[see Eq. (6.8)] and some approximations give

$$F_{n,j} = F_{n,j+1} + \tfrac{1}{2}(j+2) F_{n-1,j-2}, \tag{6.42}$$

where $F_{0,0}=1$ and

$$A_n^1 = (-1)^{n+1} \frac{8\sqrt{2}}{\pi} F_{n,1}$$

[see Eq. (6.14)].

Instead of solving Eq. (6.42) let us consider a one-parameter family of such equations. Let M be arbitrary and $F_{0,0}=1$. Then we solve

$$F_{n,j} = F_{n,j+1} + \tfrac{1}{2}(j+M) F_{n-1,j-2} \tag{6.43}$$

by introducing the generating functions

$$F(x) = \sum_{n=1}^{\infty} \frac{x^{n-1}}{(n-1)!} F_{n,1} \tag{6.44a}$$

and

$$G(x,y) = \sum_{n=1}^{\infty} \frac{x^n}{n!} \sum_{j=1}^{2n} y^{j+M+2} F_{n,j}. \tag{6.44b}$$

The analog of Eq. (6.17) is

$$\frac{\partial}{\partial x} G(x,y) + \frac{y^4}{2(1-y)} \frac{\partial}{\partial y} G(x,y) = \frac{y^{M+3}}{y-1} \left(\frac{M+2}{2} y^2 - F(x) \right). \tag{6.45}$$

Following the analysis of Secs. V C–V D, we obtain

$$F(x)\sim\frac{\Gamma[\frac{1}{2}(M+3)]}{2\sqrt{\pi}\,\Gamma[\frac{1}{2}(M+2)]}\left(\tfrac{1}{3}-x\right)^{-(M+3)/2}, \tag{6.46}$$

which is the generalization of Eq. (6.33). Finally, we repeat the work of Sec. V F and find that

$$F_{n,1}=\frac{3^{n+(M+1)/2}\Gamma[n+\frac{1}{2}(M+1)]}{2\sqrt{\pi}\,\Gamma[\frac{1}{2}(M+2)]}. \tag{6.47}$$

The particular case $M=2$ in Eq. (6.42) reduces Eq. (6.47) to

$$A_n^1\sim(-1)^{n+1}\frac{12\sqrt{6}}{\pi^{3/2}}\,3^n\Gamma(n+\tfrac{3}{2}), \tag{6.48}$$

which is precisely the case $K=1$ in Eq. (4.4).

VII. LARGE-ORDER BEHAVIOR OF WICK-ORDERED PERTURBATION THEORY

It is *necessary* to Wick-order the Hamiltonian of a multidimensional field theory. Wick-ordering removes the divergence associated with the zero-point energies of the infinitely many degrees of freedom. Correspondingly, in perturbation theory, Wick-ordering removes those (divergent) diagrams having self-loops (lines with both ends connected to the same vertex). Because the anharmonic oscillator is a field theory having only *one* degree of freedom,[28] it is *not necessary* to Wick-order the Hamiltonian H in Eq. (1.4). In addition, the non-Wick-ordered diagrams in this field theory are finite and need not be eliminated. Nevertheless, to make a stronger connection with higher-dimensional field theory, we investigate the large-order behavior of the Wick-ordered perturbation series.

We begin by Wick-ordering the Hamiltonian in Eq. (1.4). To do this, we express the fields in the interaction picture in terms of creation and annihilation operators:

$$\phi=(2m)^{-1/2}(ae^{-imt}+a^\dagger e^{imt}), \tag{7.1a}$$

$$\dot{\phi}=(\tfrac{1}{2}m)^{1/2}(-iae^{-imt}+ia^\dagger e^{imt}). \tag{7.1b}$$

Then, in terms of a and $a^\dagger$, H is

$$H=m(a^\dagger a+\tfrac{1}{2})+g(2m)^{-2}(a+a^\dagger)^4. \tag{7.2}$$

The standard way to Wick-order H in Eq. (7.2) is to place all creation operators to the left of all annihilation operators.

To elucidate this definition we use the commutation relation

$$[a,a^\dagger]=1. \tag{7.3}$$

Equation (7.3) allows us to express Wick-ordered quantities simply in terms of non-Wick-ordered ones, to wit:

$$:\phi^2:=\phi^2-\frac{1}{2m}, \tag{7.4a}$$

$$:\phi^4:=\phi^4-\frac{3}{m}\phi^2+\frac{3}{4m^2}, \tag{7.4b}$$

$$:\tfrac{1}{2}\dot{\phi}^2+\tfrac{1}{2}m^2\phi^2:=\tfrac{1}{2}\dot{\phi}^2+\tfrac{1}{2}m^2\phi^2-\tfrac{1}{2}m. \tag{7.4c}$$

We now use Eq. (7.4) to rewrite the Wick-ordered Hamiltonian $:H:$ as a *new non-Wick-ordered* Hamiltonian:

$$:H:=\tfrac{1}{2}\dot{\phi}^2+\tfrac{1}{2}m^2\phi^2-\tfrac{1}{2}m+\lambda\phi^4-\left(\frac{6\lambda}{m^3}\right)\frac{m^2\phi^2}{2}+\frac{3\lambda}{4m^2}. \tag{7.5}$$

Comparing Eq. (7.5) with Eq. (1.4) shows that Wick-ordering is equivalent to the replacement

$$m^2\to m^2(1-6\lambda/m^3), \tag{7.6a}$$

$$E\to E-\tfrac{1}{2}m+\tfrac{3}{4}m\lambda/m^3. \tag{7.6b}$$

From Eqs. (7.6) and (1.7), it follows that we can immediately express the perturbation series for the Kth energy level of the Wick-ordered Hamiltonian in terms of the Rayleigh-Schrödinger coefficients for the non-Wick-ordered Hamiltonian:

$$E_{\text{Wick}}^K\sim-\tfrac{1}{2}m+\tfrac{3}{4}m\Lambda+m(K+\tfrac{1}{2})(1-6\Lambda)^{1/2}+m\sum_{n=1}^{\infty}A_n^K\Lambda^n(1-6\Lambda)^{1/2-3n/2}, \tag{7.7}$$

where $\Lambda=\lambda m^{-3}$.

Using the binomial expansion,

$$(1-6\Lambda)^{1/2-3n/2}=\sum_{j=0}^{\infty}\frac{(6\Lambda)^j\Gamma(\frac{3}{2}n-\frac{1}{2}+j)}{j!\,\Gamma(\frac{3}{2}n-\frac{1}{2})}, \tag{7.8}$$

we simplify Eq. (7.7) to read[29]

$$E_{\text{Wick}}^K\sim mK+\tfrac{3}{2}K(K-1)m\Lambda+m\sum_{n=2}^{\infty}\Lambda^nB_n, \tag{7.9}$$

where

$$B_n^K=\sum_{j=0}^{n}\frac{A_{n-j}^K6^j\Gamma(\frac{3}{2}n-\frac{1}{2}j-\frac{1}{2})}{j!\,\Gamma(\frac{3}{2}n-\frac{3}{2}j-\frac{1}{2})}. \tag{7.10}$$

[In Eq. (7.10), $A_0^K=K+\frac{1}{2}$.] Equations (7.9) and (7.10) are exact.

We proceed to compute the large-order behavior of B_n^K. To do this, we observe that for large n, the dominant contribution to the sum in Eq. (7.10) comes from the small-j terms. We thus approximate[30]

$$\frac{\Gamma(\frac{3}{2}n-\frac{1}{2}j-\frac{1}{2})}{\Gamma(\frac{3}{2}n-\frac{3}{2}j-\frac{1}{2})}\sim(\tfrac{3}{2}n)^j\left(1-\frac{2j(j+1)}{3n}+\frac{j(j-1)(12j+11)(j+1)}{54n^2}+O(1/n^3)\right). \tag{7.11}$$

As will be seen, it is most productive to compute the large-n behavior of the ratio A_n^K/B_n^K. Equations (7.10) and (7.11) give

$$\frac{B_n^K}{A_n^K} \sim \sum_{j=0}^{N} \frac{(9n)^j}{j!} \frac{A_{n-j}^K}{A_n^K} \left(1 - \frac{2j(j+1)}{3n} + \frac{j(j-1)(12j+11)(j+1)}{54n^2} + O(1/n^3)\right) . \tag{7.12}$$

Next, we refer to Eq. (5.23) and determine[30] that for large n

$$\frac{A_{n-j}^K}{A_n^K} \sim \frac{1}{(-3n)^j}\left(1 + \frac{j^2 - 2jK}{2n} + \frac{-j(\frac{95}{3} + 58K + 34K^2) + j(j+1)(12K^2 - 12Kj + 3j^2 + j - 1)}{24n^2} + O(1/n^3)\right) . \tag{7.13}$$

Note that even though we have only determined the large-n behavior of A_n^K up to terms of order $1/n^2$ we can still calculate the ratio in Eq. (7.13) up to terms of order $1/n^3$. This is the reason why we have chosen to approximate the ratio.

Finally, we combine Eqs. (7.12) and (7.13) and allow the summation index to run from zero to ∞ to obtain

$$\frac{B_n^K}{A_n^K} \sim \sum_{j=0}^{\infty} \frac{(-3)^j}{j!}\left(1 - \frac{j^2 + 4j + 6Kj}{6n} + j\,\frac{3j^3 + 8j^2 - 48j - 338 - 522K - 306K^2 + 36Kj(j+1) + 108K^2(j+1)}{216n^2} + O(1/n^3)\right) . \tag{7.14}$$

By repeatedly shifting the summation index, we do the indicated sums in Eq. (7.14) exactly. We obtain

$$\frac{B_n^K}{A_n^K} = e^{-3}\left(1 + \frac{1+3K}{n} + \frac{\frac{71}{6} + 31K + 23K^2}{4n^2} + O(1/n^3)\right) . \tag{7.15}$$

This is the desired result which was also given in Sec. I.

To compare this prediction with our numerical results, we let $K=0$ in Eq. (7.15), take the reciprocal, and get[31]

$$\frac{A_n^0}{B_n^0} = e^3\left(1 - \frac{1}{n} - \frac{47}{24n^2} + O(1/n^3)\right) . \tag{7.16}$$

We have calculated the ratio A_n^0/B_n^0 to 74th order in perturbation theory on a computer and find that

$$\left(\frac{A_{74}^0}{B_{74}^0}\right)_{\text{computer}} = 19.806\,55 . \tag{7.17}$$

The agreement between the theoretical result in Eq. (7.16) and the computer output in Eq. (7.17) is most impressive:

$$e^3 = 20.085\,537 , \tag{7.18a}$$

$$e^3(1 - 74^{-1}) = 19.814\,111 , \tag{7.18b}$$

$$e^3[1 - 74^{-1} - 47\cdot 24^{-1}\cdot 74^{-2}] = 19.806\,928 . \tag{7.18c}$$

Despite the excellent results of Eq. (7.15) we point out that our derivation does *not* generalize to Wick-ordered $(\lambda\phi^{2N})$ field theories with $N>2$. For these theories there is no replacement equivalent to that in Eq. (7.6). However, the general problem of finding the large-n behavior of the ratio of the Rayleigh-Schrödinger coefficients in the perturbation series for the energy levels of the $(\lambda\phi^{2N})_1$ and $(:\lambda\phi^{2N}:)_1$ theories has now been solved and will be published elsewhere.[8]

APPENDIX

We give below a derivation of Eq. (3.36) which is less careful than that given in Sec. III, but which clarifies the physical ideas and minimizes the mathematical detail. In Sec. III we took pains to show how to deal with the subdominant contribution to the wave function [the exponentially decreasing $\Phi_2(x)$]. Now that $\Phi_2(x)$ is comfortably under control, we cavalierly rederive $\mathrm{Im}E(\lambda)$ without regard to subdominance. In a future paper, where we generalize to the much more complicated and difficult problem of many coupled oscillators, we will follow the techniques of this appendix rather than those of Sec. III.

First, we use a well-known relation[32] between the imaginary part of the energy of an unstable state of a real potential and the probability current $J(x)$:

$$\mathrm{Im}E = E_2 = J(x)\Big/\int_0^x \Phi^*(x')\Phi(x')dx' , \tag{A1}$$

where

$$J(x) \equiv \frac{1}{2i}\left(-\Phi^*(x)\frac{d}{dx}\Phi(x) + \Phi(x)\frac{d}{dx}\Phi^*(x)\right). \tag{A2}$$

Equation (A1) is trivially derived by multiplying Eq. (3.2) by $\Phi^*(x)$, subtracting the complex conjugate of this result, integrating from $-x$ to x, where $x > x_1$, and using the invariance of the potential under reflections $x \to -x$. (We integrate past x_1, the distant turning point, so that there is no point between x and ∞ where the current will be reflected back toward $x=0$. Thus the amount of outward probability current flow is a measure of the decay rate of the unbound state.) Note that by conservation of probability current the right-hand side of Eq. (A1) does not depend on x.

Second, we approximate the denominator of Eq. (A1) as follows: For $x<x_1$, we can replace Φ in the integral with $\mathrm{Re}\Phi$ because $\mathrm{Im}\Phi$ is small, as was shown in Sec. III. Moreover, we can approximate $\mathrm{Re}\Phi$ by $\Phi_{1A}=D_K(x)$ [see Eq. (3.8)], because $\mathrm{Re}\Phi$ and Φ_{1A} differ only in the shape of their exponentially small tails. Finally, we extend the range of integration to all positive x. Thus,[33]

$$\int_0^x \Phi^*(x')\Phi(x')dx' \sim \int_0^\infty [D_K(x')]^2 dx' = (\tfrac{1}{2}\pi)^{1/2} K\,! \,. \tag{A3}$$

Third, we evaluate $J(x)$ in Eq. (A2). We will do this in two distinct ways.

Method 1

We follow the approach of Sec. III until Eqs. (3.21), (3.22), and (3.24) have been established. These equations together imply the following behavior for the wave function $\Phi(x)$ when $x>x_1$:

$$\Phi(x)\sim 2^{-1/4}\epsilon^{1/8}(x-x_1)^{-1/4}\exp[-\tfrac{1}{4}i\pi-(6\epsilon)^{-1}-\tfrac{1}{2}(K+\tfrac{1}{2})\ln\tfrac{1}{4}\epsilon-\tfrac{1}{3}i\sqrt{2}\,\epsilon^{-1/4}(x-x_1)^{3/2}]\,. \tag{A4}$$

The expression in Eq. (A4) is then inserted in Eq. (A2) giving

$$J(x)\sim \tfrac{1}{2}e^{-1/3\epsilon}\left(\frac{4}{\epsilon}\right)^{K+1/2}\,. \tag{A5}$$

Method 2

Here we use a trick to circumvent the asymptotic matching at the distant turning point x_1. We thus reduce the problem to just *one* asymptotic connection. We follow Sec. III until Eqs. (3.11), (3.12), and (3.14) have been established. Equation (3.11) is the WKB approximation to Φ in region B:

$$\Phi(x)\sim C_1(x^2-\epsilon x^4-4K-2)^{-1/4} \times\exp\left(-\tfrac{1}{2}\int_{x_0}^x (x'^2-\epsilon x'^4-4K-2)^{1/2}dx'\right)\,. \tag{A6}$$

x_0 and C_1 are given in Eqs. (3.12) and (3.14). C_1 is determined by asymptotically matching $\Phi_{\mathrm{WKB}}(x)$ in Eq. (A6) to $D_K(x)$ at the boundary of regions A and B, as was done in Sec. IIIB. We would now like to allow x, the upper endpoint of the WKB integral, to be larger than x_1. But, of course, this expression for the WKB wave function is no longer valid as we pass the turning point at x_1. To avoid this difficulty we approach the point x along a path which goes around x_1: The path goes up the real axis, circles x_1 counterclockwise, and continues up the real axis until it reaches x. Along this contour, WKB gives a *good* approximation to Φ.

Fortunately, the *integral* in the WKB wave function depends only on the endpoint. Thus, for simplicity it may be taken entirely along the real axis. We then break the integral into two parts: (a) the portion below x_1 which is real and factors out of $J(x)$ as a constant, and (b) the portion above x_1 which is imaginary. To leading order [neglecting $O(x^{-2})<O(\epsilon)$ compared with $O(1)$], $J(x)$ is a real constant which we easily simplify to

$$J(x)=\tfrac{1}{2}C_1^{\,2}\exp\left(-\int_{x_0}^{x_1}(x'^2-\epsilon x'^4-4K-2)^{1/2}dx'\right)\,. \tag{A7}$$

We evaluate the integral in Eq. (A7) (Ref. 17) to obtain the same result as in Eq. (A5).

Finally, we combine Eqs. (A3) and (A5) as indicated in Eq. (A 1) and get

$$\mathrm{Im}E=E_2 =\frac{4^{K+1/2}}{K!(2\pi)^{1/2}}e^{-1/3\epsilon-K-1/2}\,, \tag{A8}$$

which agrees with Eq. (3.36).

---

*Work supported in part by the National Science Foundation under Grant No. GP 29463. A Sloan Fellow.

†Work supported in part by the U. S. Atomic Energy Commission under Contract No. AT(11-1)-3227.

[1]This paper is a sequel to C. M. Bender and T. T. Wu, Phys. Rev. Letters 27, 461 (1971).

[2]The equivalence is demonstrated in C. M. Bender and T. T. Wu, Phys. Rev. 184, 1231 (1969), Appendix A. This paper is referred to hereafter as BW.

[3]The Feynman rules are given in BW, Appendix B.

[4]A. M. Jaffe, Commun. Math. Phys. 1, 127 (1965). This paper gives references to the works of C. Hurst, W. Thirring, A. Petermann, and E. R. Caianiello, A. Campolattaro, and M. Marinaro.

[5]BW, Appendix C.

[6]For a description of this numerical analysis see BW,

Appendix E.

[7]Most of the results are given in Ref. 1. A complete treatment is given in C. M. Bender and T. T. Wu (unpublished).

[8]T. I. Banks and C. M. Bender, J. Math. Phys. 13, 1320 (1972).

[9]T. I. Banks, C. M. Bender, and T. T. Wu (unpublished).

[10]See B. Simon, Ann. Phys. (N.Y.) 58, 79 (1970), for discussion.

[11]J. J. Loeffel and A. Martin, CERN Report No. CERN-TH-1167, 1971 (unpublished).

[12]J. J. Loeffel, A. Martin, B. Simon, and A. S. Wightman, Phys. Letters 30B, 656 (1969).

[13]C. M. Bender and T. T. Wu, Phys. Rev. Letters 21, 406 (1968), and BW.

[14]An independent derivation of Eq. (7) may be found in the paper by Simon (Ref. 10).

[15]See N. Fröman and P. O. Fröman, *JWKB Approximation* (North-Holland, Amsterdam, 1965). The nature of the difficulty is that one of the two solutions of the Schrödinger equation becomes exponentially small ("subdominant," or "recessive") compared with the other in the region of the potential barrier and must be disregarded when one uses matched asymptotic expansions. The associated loss of information makes it very difficult to obtain the secular equation for the eigenvalues.

[16]*Higher Transcendental Functions*(Bateman Manuscript Project), edited by A. Erdélyi (McGraw-Hill, New York, 1953), Vol. 2, pp. 116–123. Hereafter, we label this reference BMP.

[17]See Ref. 2 for the relevant mathematical techniques for approximating the WKB integral.

[18]M. Abramowitz and I. A. Stegun, *Handbook of Mathematical Functions* (National Bureau of Standards, Washington, D. C., 1964), Eq. 10.4.1. Hereafter, we label this reference NBS.

[19]NBS, Eqs. 10.4.60 and 10.4.64.

[20]NBS, Eqs. 10.4.59 and 10.4.63.

[21]BMP, Vol. 2, p. 123, Eq. (2).

[22]There is a misprint in Eq. (3) of Ref. 1 which becomes evident when it is compared with Eq. (4.4) of this paper. In Eq. (3) the curly brackets should be raised to the $nN-n+K+\frac{1}{2}$ power (the K was omitted).

[23]See BMP, Vol. 1, Sec. (1.2), Eqs. (5) and (15).

[24]See Ref. 2, Appendix F.

[25]See Ref. 2, Appendix E, Eq. (E8a). There is a misprint in Eq. (E8): All decimals should be preceeded by a (−) sign.

[26]We are most grateful to Ken Anderson for his assistance in this difficult computer calculation. The numerical fits were obtained from a 36-place (4-fold precision) calculation of the ground state energy to 150th order in perturbation theory.

[27]This difference equation is also derived in Ref. 2, Sec. II.

[28]See Ref. 2, Appendixes A and B.

[29]To compute the coefficient of A in Eq. (7.9) it is necessary to know $A_1{}^K$. See Eq. (5.11).

[30]See NBS, p. 257, Eq. 6.1.47.

[31]There is a misprint in Ref. 1, Eq. (18). The coefficient of the n^{-2} term was given incorrectly as $-41/24$; it should be $-47/24$ as in Eq. (7.16).

[32]We credit Dr. George Zipfel as the first to use Eq. (A1) in connection with the anharmonic oscillator.

[33]See BMP, Vol. 2, Sec. (8.3), Eq. (23). There is a factor of 2 error in BMP which has been corrected in Eq. (A3).